Prediction of temperature in 2 meters temperature probe survey in Blawan geothermal field using artificial neural network (ANN) method

Akhmad Afandi [a],[*], Nuraini Lusi [a], I.G.N.B. Catrawedarma [a], Subono [b], Bayu Rudiyanto [c]

[a] *Department of Mechanical Engineering, Politeknik Negeri Banyuwangi, 68461, Banyuwangi, Indonesia*
[b] *Department of Informatic Engineering, Politeknik Negeri Banyuwangi, 68461, Banyuwangi, Indonesia*
[c] *Energy Engineering Laboratory, Department of Renewable Energy Engineering, Politeknik Negeri Jember, 68121, Jember, Indonesia*

ARTICLE INFO

ABSTRACT

Research on temperature gradient has been carried out in Blawan geothermal area. This study aims to predict the temperature in the subsurface temperature measurement using a temperature probe with a depth of 2 m in the Blawan geothermal area. Temperature and depth are the two variables being measured. Meanwhile, the resistivity, conductivity, and humidity data were taken from previous studies in the exact area measurements. The prediction determination used modeling with an Artificial Neural Network (ANN) with the back-propagation method. The optimal predictions using an Artificial Neural Network (ANN) were obtained by constructing three input layers, five hidden layers, and two output layers (3-5-2) with a hyperbolic tangent function. Results for temperature prediction with the larger R^2 (1) values and lower MAPE (1.07%), RMSE (0.78), MSE (0.61), and MAD (0.34) values. Moreover, humidity generates a greater R^2 (1) values and lower MAPE (0.34%), RMSE (0.34), MSE (0.18), and MAD (0.29) values. ANN proved very effective in predicting temperature and humidity factors.

1. Introduction

Geothermal Energy is one of the energies most countries have not utilized optimally [1]. Indonesia has 312 geothermal locations spread from Sumatra to Irian Jaya with a potential of 23.9 GW [2], and in 2013 increased by 24.02 GW [3]. Around 2130.7 MW of new geothermal power plants were installed in Indonesia in 2020, accounting for 8.9% of the country's total installed capacity [4]. One of the geothermal prospect areas in Indonesia is Blawan geothermal field, located in Rengahrejo Hamlet, Kalianyar Village, Sempol Sub-district, Bondowoso Regency, with coordinates −7.986528828, 114.174539662. The location has 21 hot springs that appear on the surface with temperatures ranging from 25 °C–50 °C [5] with an estimated potential of 10 MW [6]. Several stages of surveys are needed for geothermal energy utilization, including surveys of geothermal manifestations, geological and hydrological surveys, geochemical surveys, geophysical surveys, and the manufacture of exploration wells [7,8].

One of the geophysical methods for preliminary surveys is the thermal method. This method determines the temperature below the ground surface and detects anomalies in hot areas [8]. The thermal method measures the surface temperature to a depth of 1 m or a 1-m temperature probe survey. In addition, several probe survey studies have been carried out, including research on temperature

---

gradient [9,10] and heat transfer [11].

Researchers have installed temperature sensors at a depth of 0.4 m in the Blawan Geothermal area to conduct temperature probe investigations on the earth's surface to a depth of 2 m. Where the study's findings can be used to estimate the geothermal reservoir's temperature at a depth of 2000 m to be roughly 194 °C and its average heat flow to be 312.082 W/m^2 [10]. However, this study has not explained the validity and optimization of the measurement results read by the temperature sensor at each depth.

Artificial Neural Network (ANN) is one of the optimization methods that can predict and explain the nonlinear relationship between input and output to find patterns in the data [12], reduces linearity errors from sensor readings [13], and is more accessible than numerical methods [14]. The acceptable error limits of ANN results were obtained within 5% [15], and ANN was particularly effective in predicting the damage factor due to its high R^2 and low RMSE and MEP values [16]. Pandey and Singh explained that Artificial Neural Network (ANN) is a solution that can be applied to complex geothermal systems to solve problems that are not done with analytical solutions [17]. In the use of the Artificial Neural Network (ANN) method, many are found in the fields of animal science [18, 19], Medicine [20,21], pharmacology [22,23], and many more are found in other fields. However, it is rare to find the Artificial Neural Network (ANN) method used in geothermal.

Due to these issues, it is crucial to forecast the temperature at the 2 m temperature probe survey using the Artificial Neural Network (ANN) method because this method is excellent for forecasting soil temperature [24,25]. This way, the obtained temperature value can be helpful for future research.

2. Materials and methods

2.1. Two meters temperature probe survey

The study was conducted in Blawan hot water at a depth of 2 m with the help of a temperature sensor based on an Arduino microcontroller (Fig. 1). The temperature measurement is to determine the temperature value at each depth. The temperature sensor uses DS18B20, which is placed every 0.01-m depth up to 2 m. There are 21 sensors to detect the temperature below the ground surface (Fig. 2). Sending data is using wifi, and the data is stored on a MicroSD located in the toolbox, making it easier to retrieve data in steep areas.

The recorded temperature data is taken from the average value at each depth. The resistivity, humidity, and conductivity data were obtained from a geoelectric and pH survey in the Blawan geothermal area. So the data used are temperature, humidity, depth, resistivity, and conductivity, as in Table 1.

2.2. Artificial Neural Network (ANN)

In general, Artificial Neural Network (ANN) is formed by several neurons as an information processing unit serving as the basis for the operation of a function according to its task [26]. The fundamental element of the neural network is a neuron composed of neurons, weights inputs, a function of activation, a function of summation, and output [27,28]. Artificial Neural Network (ANN) includes a number of network topologies that are frequently utilized in their use in diverse applications, including Single-Layer nets made up of input units, one layer of weights, and output units, and Multi-Layer nets made up of input, hidden, and output. To determine the best architecture with the steps to find the best combination between input and the number of hidden. However, the Artificial Neural Network (ANN) modeling does not have a general procedure regarding the number of inputs, hidden layers, and nodes in each hidden layer.

Several activation functions are used in ANN modeling, including threshold function, step activation function, sigmoid function, and hyperbolic tangent function [16]. In this paper, we use the hyperbolic tangent function using the equation [29]:

$$\varnothing(z) = z.g(z) \tag{1}$$

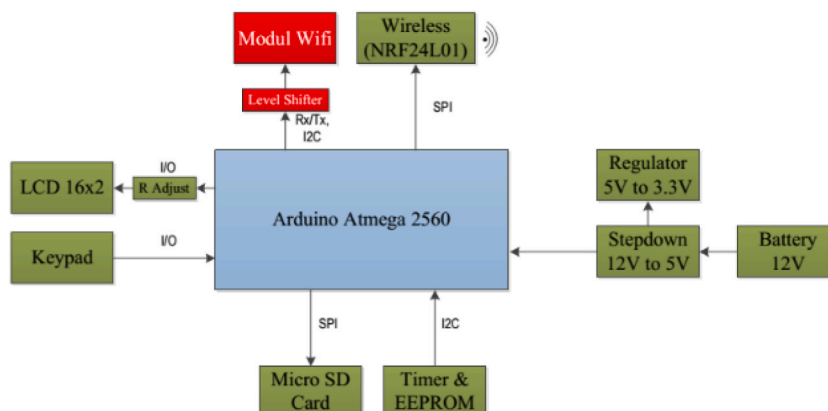where $g(z)$ is a hyperbolic tangent function and can be described by
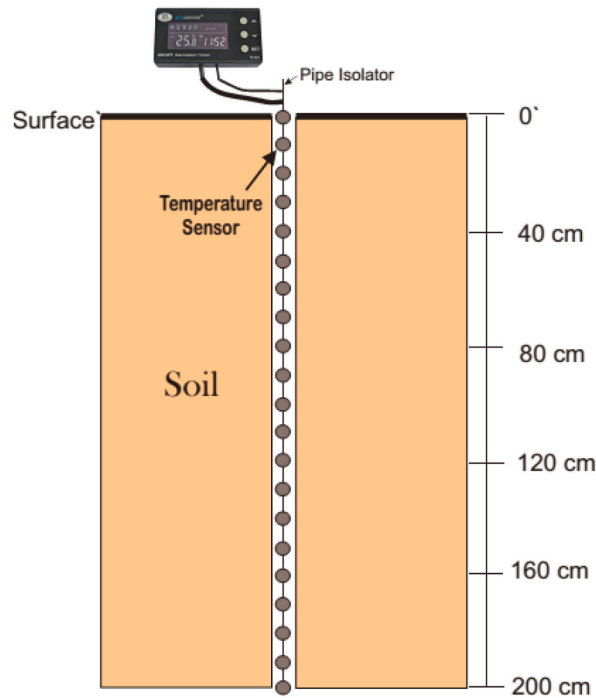

Fig. 1. Main master diagram.

Fig. 2. Temperature measurement position.

Table 1
Data acquisition results.

No	Depth (m)	Resistivity (Ω)	Conductivity (Ω^{-1})	Temperature (°C)	Humidity
1	0	2	0.5	24.38	83,4
2	0.1	3	0.3333	25.56	85,2
3	0.2	4	0.25	25.63	85,3
4	0.3	6	0.1667	25.69	85,6
5	0.4	8	0.125	25.94	86,1
6	0.5	10	0.1	31.06	87,6
7	0.6	16	0.0625	34.94	88,2
8	0.7	26	0.0385	35.06	88,7
9	0.8	32	0.0313	35.13	88,9
10	0.9	48	0.0208	35.19	88,9
11	1	54	0.0185	32.69	88,1
12	1.1	64	0.0156	36.00	89,2
13	1.2	76	0.0131	36.06	89,2
14	1.3	82	0.0121	36.13	89,4
15	1.4	114	0.0088	35.94	89,6
16	1.5	128	0.0078	35.25	89,3
17	1.6	156	0.0064	35.94	89,8
18	1.7	196	0.0051	36.19	91,2
19	1.8	210	0.0048	36.25	91,4
20	1.9	228	0.0044	36.35	91,6
21	2	256	0.0039	36.50	91,6

$$g(z) = Tanh\ (z) = \frac{exp^z - exp^{-z}}{exp^z + exp^{-z}} \qquad (2)$$

where (z) is the input to the activation function, and *exp* is the exponential function.

The value (weight) of the interaction between the neurons in the ANN determines the output, which takes the shape of a certain input pattern. The ANN will solve complex problems using appropriate values (weights) between neurons in different layers. Thus, one of the steps that must be taken is the training process [30]. The mechanism in supervised training is often called back-propagation (BP) (Fig. 3), and this application is widely used in the engineering field. The back-propagation algorithm was constructed in the ANN modeling to optimize the training model in the selection process [27].

The network training rules for backpropagation consist of two stages: feedforward and backward propagation. On the network is
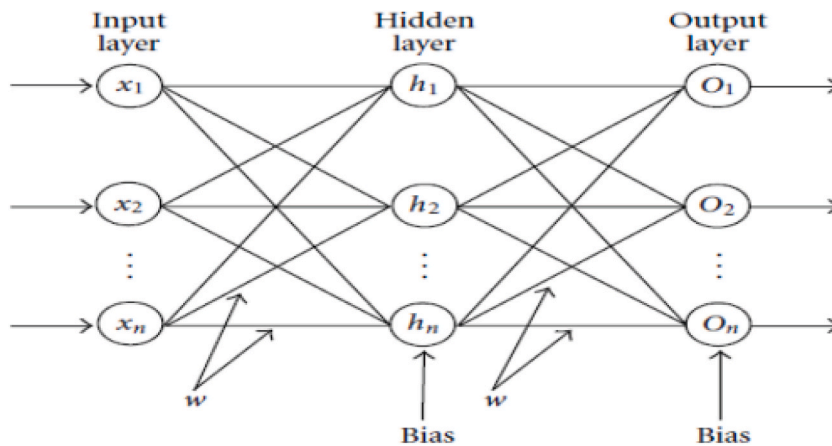
Fig. 3. Backpropagation Algorithm Artificial Neural Network Architecture [32].

given a set of training examples called training sets. This training set is represented by a feature vector called the associated input vector with an output that is the target of the training. In other words, the training set consists of an input vector and a target output vector. Exodus from the network is an actual output vector. Next, a comparison is made between the actual output produced and the target output by reducing the two outputs. The result of the reduction is an error. Errors are used to make changes to each weight by re-propagating it. Any weight changes that occur can reduce errors. Cycle weight changes (epochs) are carried out in each training set so that the 30 stop is reached. When the set number of epochs is reached or when a set threshold value is passed. The backpropagation network training algorithm consists of 3 stages that are [31]:

1. The feedforward stage

   The input layer is first calculated by summing the weight and bias values up to the output layer using a predetermined activation function.

2. The stage of feedback (backpropagation)

   Calculate the difference between network output with the desired target, which is then referred to as an error. Next is the back-propagation phase, the error factor is propagated backward, starting from the corresponding line directly with the units in the output layer.

3. The stage of updating the weights and biases

   The last phase is modifying the weights to reduce errors that occurred.

   At the same time, the network architecture used in this study is a multi-layer net having three layers, namely input, hidden, and output (Fig. 4). By using the hyperbolic tangent function to find the optimum number of neurons in the training and testing data (R Square (R^2), Root Average Squared Error (RASE), and Mean Absolute Deviation (MAD)).

   To calculate the percentage of error prediction results that have been obtained, using the prediction error percentage equation, then using equation (3) [30]. The prediction error percentage is the result of subtracting the predicted value from the actual value and dividing by the actual value, and the result is multiplied by 100%.
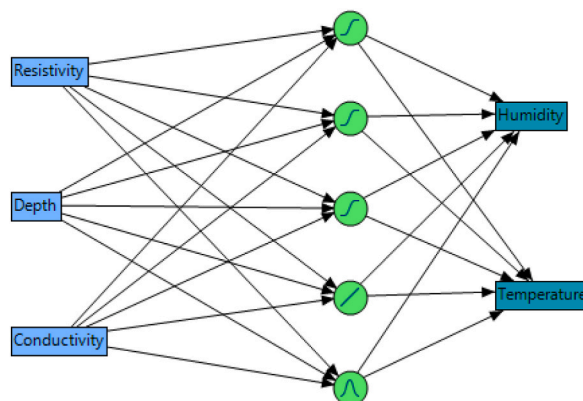

Fig. 4. Schematic of the ANN diagram used.

$$\% \ error = \frac{|predicted \ value - measured \ value|}{measured \ value} x100 \tag{3}$$

2.3. Statistical accuracy measurement

The accuracy of forecasting results is a measure of forecasting error indicating the degree of difference between the results of demand forecasting and the demand happened [33]. In all instances involving forecasting, there is a degree of uncertainty. The variation in the forecast is not only the element of the mistake but also the forecasting model's incapacity to distinguish other data series elements. Consequently, the magnitude of the forecasting results variation can be due to unforeseen causes (outliers). The validation of forecasting methods cannot be separated from indicators in measuring forecasting accuracy. There are some indicators for measuring the accuracy of forecasting, but the most commonly used are Mean Absolute Percentage Error (MAPE), Root Mean Square Error (RMSE), Mean Square Error (MSE), and Mean Absolute Deviation (MAD). Forecasting accuracy will be high if the values of it are getting smaller.

Meanwhile, to determine the accuracy and precision value in the optimization results, it is used statistical equations including:

a) Mean Absolute Percentage Error (MAPE)

Mean Absolute Percentage Error (MAPE) is a relative determination model that determines the percentage value of deviations from the estimation results [34]. The equations used are like equation (4).

$$MAPE = \frac{1}{N} \sum_{t=1}^{n} \left| \frac{A_t - F_t}{A_t} \right| \tag{4}$$
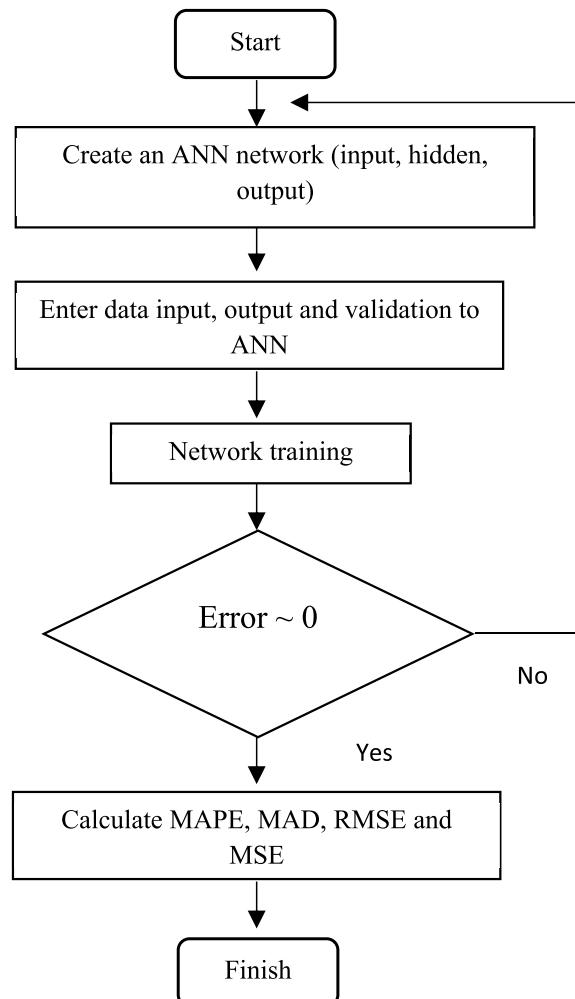
where: A_t = Actual.

Fig. 5. Flowchart of research.

F_t = Forecast

b) Root Mean Square Error (RMSE)

Root Mean Square Error (RMSE) is the square root of Mean Square Error (MSE) [35]. The equations used can be seen in equation 5

$$RMSE = \sqrt{\frac{\sum_{t=1}^{n}(A_t - F_t)^2}{n}}$$

(5)

where: A_t = Actual.

F_t = Forecast

c) Mean Square Error (MSE)

Mean Square Error (MSE) is the error value obtained from the average square of the subtraction between the actual value and the estimated value [36]. The equations used can be seen in equation (6).

$$MSE = \frac{\sum_{t=1}^{n}(A_t - F_t)^2}{n}$$

(6)

where: A_t = Actual.

F_t = Forecast

d) The mean absolute deviation (MAD)

The mean absolute deviation (MAD) is the sum of the absolute differences between the actual and estimated values divided by the number of observations or what is known as the mean absolute deviation [37]. The equations used can be seen in equation 7

$$MAD = \frac{\sum_{t=1}^{n}|A_t - F_t|}{n}$$

(7)

where: A_t = Actual.

F_t = Forecast

As for the flowchart in this study, as shown in Fig. 5.

3. Results and discussion

Artificial Neural Network (ANN) is a method that is often used to predict temperatures in geothermal, the use of Artificial Neural Network (ANN) structures is needed to estimate output based on a good interpolation scheme [38]. The experimental parameters are listed in Table 1, and they are as follows: temperature, depth, resistivity, conductivity, and humidity. In this model, depth, resistivity, and conductivity serve as inputs, whereas temperature and humidity play the roles of outputs.

Statistical data of the optimum number of neuron's temperatures (Table 2) and statistical data of the optimum number of neuron's humidity (Table 3), modeling is done by making a trial error to find the construction of the ANN diagram with the best validation value so that the structure of three input layers, five hidden layers, and two output layers is obtained (Fig. 4). The results of the resulting temperature prediction are as in Table 4, and humidity prediction is as in Table 5.

A linear regression graph can be made between the actual temperature value and the predicted temperature based on Table 4 (Fig. 6). The linear equation y = 0.9828x + 0.7463 is obtained, and the coefficient of determination (R^2) is 0.9703. The coefficient value indicates that the ANN-based prediction value is extremely accurate and that there is a strong correlation between the actual temperature variable and the predicted temperature.

The predicted value is obtained at the humidity output as in Table 5. The actual and predicted values are almost identical, as seen in Fig. 7. The linear equation obtained is y = 0.9069x + 8.3225 with a coefficient of determination (R^2) of 0.9684. The value of the coefficient shows that the ANN prediction is very accurate and that the relationship between the actual temperature variable and the

Table 2
Statistical data of the optimum number of neuron's temperature.

Number of Neuron	Learning rate	Temperature					
		Training Data			Testing Dara		
		R^2	RASE	MAD	R^2	RASE	MAD
3-3-2	0.1	0.89	1.42	0.82	0.89	1.55	1.01
3-4-2	0.1	0.82	2.41	1.25	0.76	2.23	1.65
3-5-2	0.1	0.99	0.19	0.11	0.91	1.31	0.85
3-6-2	0.1	0.92	1.58	0.82	0.83	1.77	1.4
3-7-1	0.1	0.8	2.23	1.33	0.72	2.36	1.82
3-8-2	0.1	0.84	2.19	1.19	0.72	2.31	1.7

Table 3
Statistical data of the optimum number of neuron's humidity.

Number of Neuron	Learning rate	Humidity					
		Training Data			Testing Dara		
		R^2	RASE	MAD	R^2	RASE	MAD
3-3-2	0.1	0.97	0.36	0,3	0,94	0,39	0,25
3-4-2	0.1	0.94	0.57	0.39	0.95	0.37	0.31
3-5-2	0.1	0.98	0.29	0.23	0.94	0.39	0.23
3-6-2	0.1	0.97	0.46	0.27	0.83	0.68	0.55
3-7-2	0.1	0.94	0.52	0.37	0.95	0.45	0.28
3-8-2	0.1	0.98	0.35	0.23	0.82	0.72	0.57

Table 4
Actual temperature value and predicted temperature.

No	Actual Temperature (^{o}C)	Predicted Temperature (^{o}C)
1	24.38	25.27
2	25.56	25.57
3	25.63	25.31
4	25.69	25.66
5	25.94	25.94
6	31.06	31.06
7	34.94	34.93
8	35.06	34.92
9	35.13	35.11
10	35.19	35.83
11	32.69	35.99
12	36.00	36.08
13	36.06	36.01
14	36.13	35.90
15	35.94	35.59
16	35.25	35.68
17	35.94	35.84
18	36.19	35.87
19	36.25	36.13
20	36.35	36.42
21	36.50	36.55

Table 5
Actual humidity value and predicted humidity.

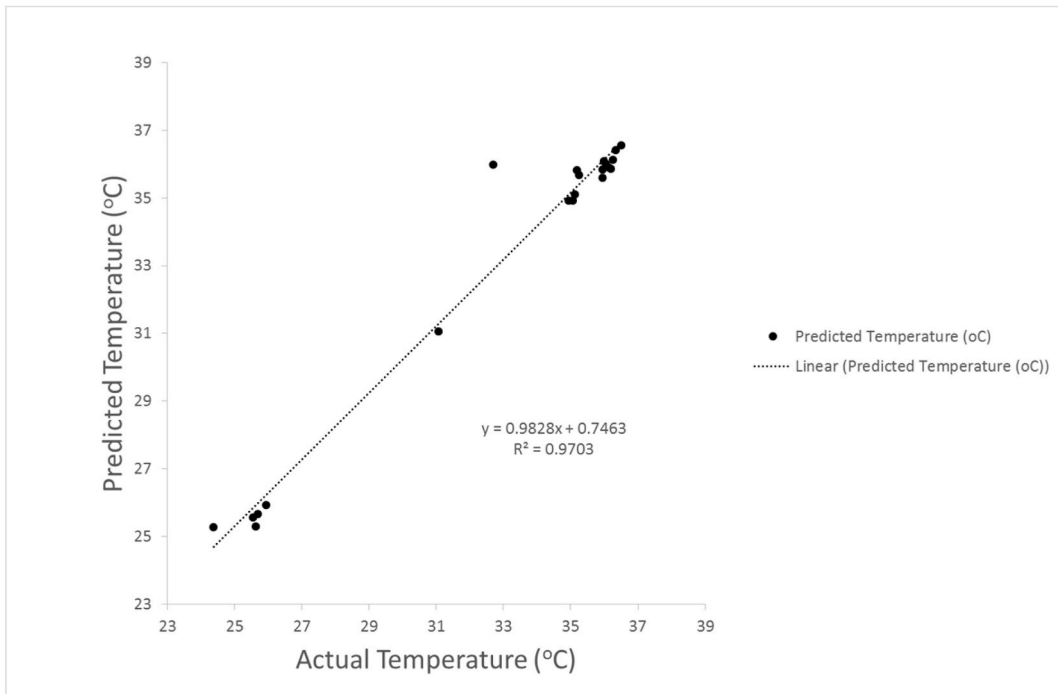| No	Actual Humidity	Predicted Humidity
1	83.4	84.68
2	85.2	85.05
3	85.3	85.35
4	85.6	85.73
5	86.1	86.19
6	87.6	87.36
7	88.2	88.33
8	88.7	88.84
9	88.9	88.93
10	88.9	89.12
11	88.1	88.97
12	89.2	89.09
13	89.2	89.18
14	89.4	89.32
15	89.6	89.43
16	89.3	89.77
17	89.8	90.13
18	91.2	90.52
19	91.4	90.92n
20	91.6	91.32
21	91.6	91.88

Fig. 6. Regression of actual temperature and predicted temperature.
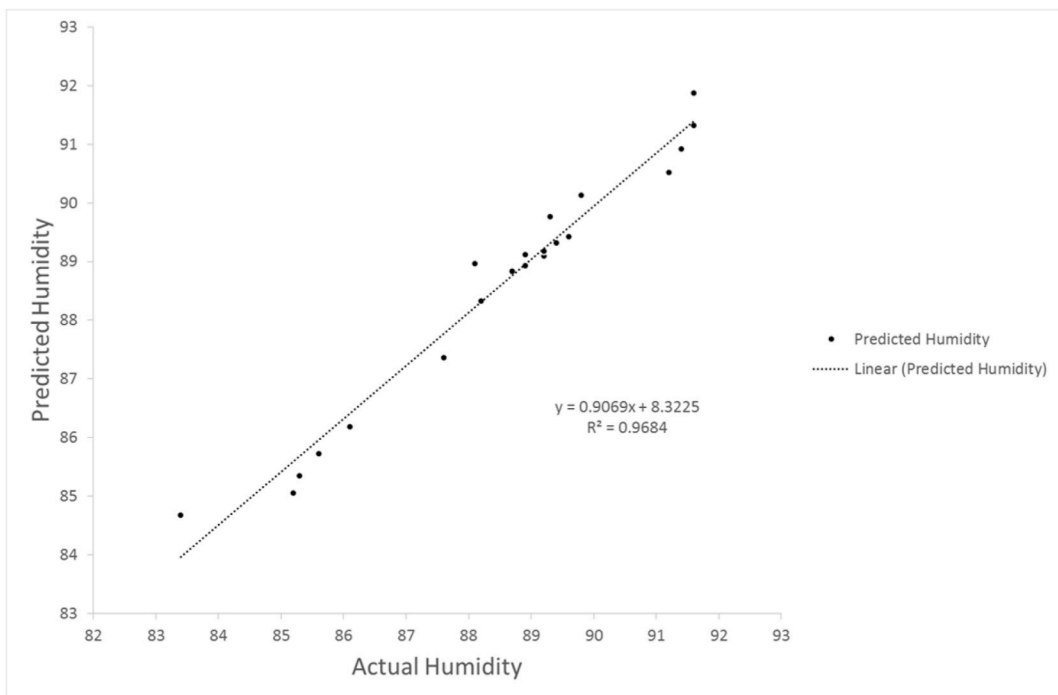

Fig. 7. Regression of actual humidity and predicted humidity.

predicted temperature is robust.

Table 6 shows the percentage prediction error to determine the error percentage for each actual temperature and predicted temperature. The results were obtained in Table 6 with an average Percentage Prediction Error of 0.034% using equation (3). Fig. 8 shows a linear regression graph with a value of y = 0.1x+2E-7 with a coefficient of determination (R^2) of 1. In addition, Table 6 can

Table 6
Calculation results of Percentage Prediction Error of Temperature.

No	Actual Temperature (°C)	Predicted Temperature (°C)	Percentage Prediction Error (%)
1	24.38	25.27	0.089
2	25.56	25.57	0.001
3	25.63	25.31	0.032
4	25.69	25.66	0.003
5	25.94	25.94	0.000
6	31.06	31.06	0.000
7	34.94	34.93	0.001
8	35.06	34.92	0.014
9	35.13	35.11	0.002
10	35.19	35.83	0.064
11	32.69	35.99	0.330
12	36.00	36.08	0.008
13	36.06	36.01	0.005
14	36.13	35.90	0.023
15	35.94	35.59	0.035
16	35.25	35.68	0.043
17	35.94	35.84	0.010
18	36.19	35.87	0.032
19	36.25	36.13	0.012
20	36.35	36.42	0.007
21	36.50	36.55	0.005
Average			0.034

also explain the optimum results to describe the optimum between the actual temperature (31.06 °C) and the predicted temperature (31.06 °C) with a depth of 0.5 m, resistivity 10 Ω, and a conductivity value of 0.1 Ω^{-1}.

Table 7 shows the percentage prediction error to determine the error percentage for each actual humidity and predicted humidity. The results were obtained in Table 7 with an average Percentage Prediction Error of 0.03% using equation (3). Table 7 shows a linear regression graph with a value of y = 0.1x with a coefficient of determination (R^2) of 1 (Fig. 9). In addition, Table 7 can also explain the optimum results to describe the optimum between the actual humidity (85.3) and the predicted humidity (85.35) with a depth of 0.2 m, resistivity 4 Ω, and a conductivity value of 0.25 Ω^{-1}.

Calculating the mean absolute percent error (MAPE), mean square error (MSE), mean absolute deviation (MAD) [39], and root mean square error (RMSE) on the actual temperature value and the forecasted temperature value is required to compare the results above. The results of these calculations are as in Table 8.

In Table 8, the Mean Absolute Percentage Error (MAPE) value of temperature and humidity is 1.07 and 0.34. These results can be interpreted that the temperature prediction is accurate because Caraka et al. explained that the MAPE value <4.9% is very accurate [40]. Meanwhile, for the Mean Square Error (MSE) and the Root Mean Square Error (RMSE), the values obtained are almost close to 0 (0.61 and 0.78) for temperature and 0.18 and 0.34 for humidity, so it can be interpreted that these values are by the actual data. Meanwhile, for the mean absolute deviation (MAD), the result of 0.34 and 0.29 (Temperature and Humidity) can be interpreted as a
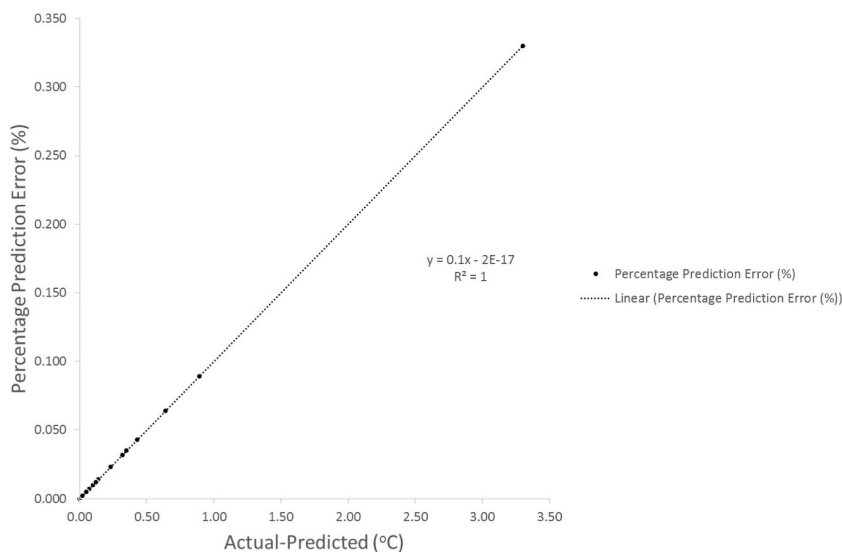

y = 0.1x - 2E-17
R² = 1

● Percentage Prediction Error (%)
······· Linear (Percentage Prediction Error (%))

Fig. 8. Regression percentage prediction error of temperature.

Table 7
Calculation results of Percentage Prediction Error of Humidity.

| No	Actual Humudity	Predicted Humidity	Percentage Prediction Error (%)
1	83.4	84.68	0.128
2	85.2	85.05	0.015
3	85.3	85.35	0.005
4	85.6	85.73	0.013
5	86.1	86.19	0.009
6	87.6	87.36	0.024
7	88.2	88.33	0.013
8	88.7	88.84	0.014
9	88.9	88.93	0.003
10	88.9	89.12	0.022
11	88.1	88.97	0.087
12	89.2	89.09	0.011
13	89.2	89.18	0.002
14	89.4	89.32	0.008
15	89.6	89.43	0.017
16	89.3	89.77	0.047
17	89.8	90.13	0.033
18	91.2	90.52	0.068
19	91.4	90.92	0.048
20	91.6	91.32	0.028
21	91.6	91.88	0.028
Average			0.03
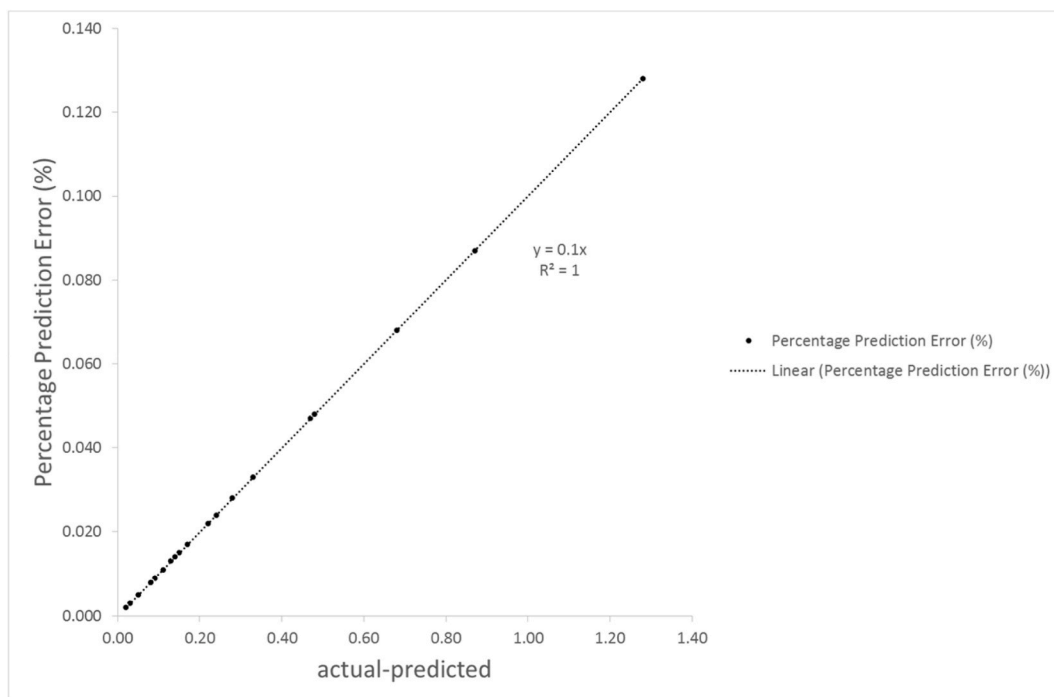
Fig. 9. Regression percentage prediction error of humidity.

Table 8
The results of calculating the level of accuracy.

Stats Items	The calculation results	
	Temperature	Humidity
MAPE	1.07	0.34
MSE	0.61	0.18
MAD	0.34	0.29
RMSE	0.78	0.34

value that has minimal error and a good level of accuracy.

4. Conclusion

The ANN model with the back-propagation method can be applied in predicting the temperature of the subsurface temperature measurement using a temperature probe with a depth of 2 m in the geothermal Blawan area, shown through the validation results. The parameters were used to give perfect results.

1. The performance of the ANN model shows that the multi-layer net model with the 3-5-2 architecture gives the most optimum with a hyperbolic tangent function, and the learning rate is 0.1. The value of R^2 on the training data is 0.99, and the testing data is 0.91. The RASE on the training data is 0.19, and the testing data is 1.31. Training data on MAD is 0.11, and testing data is 0.85 (temperature). The value of R^2 on the training data is 0.98, and the testing data is 0.94. The RASE on the training data is 0.29, and the testing data is 0.39. Training data on MAD is 0.23, and testing data is 0.23 (humidity).
2. The actual temperature and the temperature predicted value are obtained by the linear regression equation $y = 0.9828x + 0.7463$ with a coefficient of determination (R^2) of 0.9703. While the regression equation on the percentage prediction error gets the equation $y = 0.1x+2E-7$ with an average error value of 0.034% and a coefficient of determination (R^2) of 1. The actual humidity and the humidity predicted value are obtained by the linear regression equation $y = 0.9069x + 8.3225$ with a coefficient of determination (R^2) of 0.9684. While the regression equation on the percentage prediction error gets the equation $y = 0.1x$ with an average error value of 0.03% and a coefficient of determination (R^2) of 1. From these coefficient values, it can be interpreted that the prediction value using ANN is very accurate, and the relationship between the actual temperature variable and the predicted temperature is very strong.
3. The statistical test process to obtain accuracy and precision from the optimization results using MAPE, MSE, MAD, and RMSE obtained values of 1.07%, 0.61, 0.34, and 0.78 (temperature), and 0.34%, 0.18, 0.29, and 0.34 (Humidity). The conclusion has very small errors and good levels of accuracy and precision.

Authorship contributions

Category 1: Conception and design of study: Akhmad Afandi, IGNB Catrawedarma, Bayu Rudiyanto; acquisition of data: Akhmad Afandi, Subono, Nuraini Lusi; analysis and/or interpretation of data: Akhmad Afandi, Nuraini Lusi, IGNB Catrawedarma, Bayu Rudiyanto.

Category 2: Drafting the manuscript: Akhmad Afandi, Nuraini Lusi, Subono, IGNB Catrawedarma; revising the manuscript critically for important intellectual content: Akhmad Afandi, Nuraini Lusi, IGNB Catrawedarma, Bayu Rudiyanto.

Category 3: Approval of the version of the manuscript to be published (the names of all authors must be listed):Akhmad Afandi, IGNB Catrawedarma, Subono, Bayu Rudiyanto.

Declaration of competing interest

The authors declare that they have no known competing financial interests or personal relationships that could have appeared to influence the work reported in this paper.

Data availability

The data that has been used is confidential.

Acknowledgment

References

[1] J.R. Patterson, M. Cardiff, K.L. Feigl, Optimizing geothermal production in fractured rock reservoirs under uncertainty, Geothermics 88 (2020), 101906.
[2] N.A. Pambudi, Geothermal power generation in Indonesia, a country within the ring of fire: current status, future development and policy, Renew. Sustain. Energy Rev. 81 (2018) 2893–2901.
[3] A. Fauzi, Geothermal resources and reserves in Indonesia: an updated revision, Geotherm. Energy Sci. 3 (1) (2015) 1–6.
[4] D.J.E. Kementerian Energi dan Sumber Daya Mineral, Laporan Kinerja EBTKE, 2020.
[5] S. Maryanto, et al., Magnetotelluric-geochemistry investigations of blawan geothermal field, East Java, Indonesia, Geosciences 7 (2) (2017) 41.
[6] A. Afandi, S. Maryanto, A. Rachmansyah, Identifikasi reservoar daerah panasbumi dengan metode geomagnetik daerah blawan kecamatan Sempol kabupaten Bondowoso, J. Neutrino J. Fis. dan Apl. (2013) 1–10.
[7] E. Barbier, Geothermal energy technology and current status: an overview, Renew. Sustain. Energy Rev. 6 (1–2) (2002) 3–65.
[8] H.K. Gupta, S. Roy, Geothermal Energy: an Alternative Resource for the 21st Century, Elsevier, Amsterdam, 2006.
[9] M.F. Coolbaugh, C. Sladek, J.E. Faulds, R.E. Zehner, G.L. Oppliger, Use of rapid temperature measurements at a 2-meter depth to augment deeper temperature gradient drilling, in: Thirty-second Workshop on Geothermal Reservoir Engineering, 2007.
[10] A. Afandi, N. Lusi, S.D.A. Febriani, Prediction of the distribution of geothermal sources based on the geothermal temperature gradient in the Blawan Bondowoso, Case Stud. Therm. Eng. 25 (2021), 100931.
[11] B.E.B. Nurhandoko, et al., Accurate thermal conductivity measurement of Java and Sumatra rock samples using time varying heat flow measurement, IOP Conf. Ser. Earth Environ. Sci. 311 (1) (2019), 12045.

[12] X. Fang, N. Papaioannou, F. Leach, M.H. Davy, On the application of artificial neural networks for the prediction of NO x emissions from a high-speed direct injection diesel engine, Int. J. Engine Res. 22 (6) (2021) 1808–1824.
[13] T.T.K. Tran, S.M. Bateni, S.J. Ki, H. Vosoughifar, A review of neural networks for air temperature forecasting, Water 13 (9) (2021) 1294.
[14] V.N. Kumar, K.V.L. Narayana, Development of thermistor signal conditioning circuit using artificial neural networks, IET Sci. Meas. Technol. 9 (8) (2015) 955–961.
[15] F. Kara, K. Aslantas, A. Çiçek, ANN and multiple regression method-based modelling of cutting forces in orthogonal machining of AISI 316L stainless steel, Neural Comput. Appl. 26 (1) (2015) 237–250.
[16] Ö. Erkan, B. Işık, A. Çiçek, F. Kara, Prediction of damage factor in end milling of glass fibre reinforced plastic composites using artificial neural network, Appl. Compos. Mater. 20 (4) (2013) 517–536.
[17] S.N. Pandey, M. Singh, Artificial neural network to predict the thermal drawdown of enhanced geothermal system, J. Energy Resour. Technol. 143 (January) (2021) 1–8.
[18] C. Fernández, E. Soria, J.D. Martin, A.J. Serrano, Neural networks for animal science applications: two case studies, Expert Syst. Appl. 31 (2) (2006) 444–450.
[19] W. Grzesiak, R. Lacroix, J. Wójcik, P. Blaszczyk, A comparison of neural network and multiple regression predictions for 305-day lactation yield using partial lactation records, Can. J. Anim. Sci. 83 (2) (2003) 307–310.
[20] Q.K. Al-Shayea, Artificial neural networks in medical diagnosis, Int. J. Comput. Sci. Issues 8 (2) (2011) 150–154.
[21] R. Dey, V. Bajpai, G. Gandhi, B. Dey, Application of artificial neural network (ANN) technique for diagnosing diabetes mellitus, in: IEEE Region 10 and the Third International Conference on Industrial and Information Systems, 2008, pp. 1–4, 2008.
[22] A. Bucinski, A. Nasal, R. Kaliszan, Pharmacological classification of drugs based on neural network processing of molecular modeling data, Comb. Chem. High Throughput Screen. 3 (6) (2000) 525–533.
[23] M.C. Grassi, A.M. Caricati, M. Intraligi, M. Buscema, P. Nencini, Artificial neural network assessment of substitutive pharmacological treatments in hospitalised intravenous drug users, Artif. Intell. Med. 24 (1) (2002) 37–49.
[24] S. Zhou, X. Chu, S. Cao, X. Liu, Y. Zhou, Prediction of the ground temperature with ANN, LS-SVM and fuzzy LS-SVM for GSHP application, Geothermics 84 (2020), 101757.
[25] H.Z. Abyaneh, M.B. Varkeshi, G. Golmohammadi, K. Mohammadi, Soil temperature estimation using an artificial neural network and co-active neuro-fuzzy inference system in two different climates, Arabian J. Geosci. 9 (5) (2016) 377.
[26] L. Fausset, Fundamentals of Neural Network: Architectures, Algorithms and Applications, Prentice Hall, 1994.
[27] A. Eser, E. Aşkar Ayyıldız, M. Ayyıldız, and F. Kara, "Artificial intelligence-based surface roughness estimation modelling for milling of AA6061 alloy," Adv. Mater. Sci. Eng., vol. 2021, 2021.
[28] F. Kara, M. Karabatak, M. Ayyıldız, E. Nas, Effect of machinability, microstructure and hardness of deep cryogenic treatment in hard turning of AISI D2 steel with ceramic cutting, J. Mater. Res. Technol. 9 (1) (2020) 969–983.
[29] S.K. Roy, S. Manna, S.R. Dubey, B.B. Chaudhuri, LiSHT: Non-parametric Linearly Scaled Hyperbolic Tangent Activation Function for Neural Networks, 2019 *arXiv Prepr. arXiv1901.05894*.
[30] W. Guang, M. Baraldo, M. Furlanut, Calculating percentage prediction error: a user's note, Pharmacol. Res. 32 (4) (1995) 241–248.
[31] A. Cripps, Using artificial neural nets to predict academic performance, in: Proceedings of the 1996 ACM Symposium on Applied Computing, 1996, pp. 33–37.
[32] A. Goel, ANN-based approach for predicting rating curve of an Indian River, Int. Sch. Res. Notices (2011) 2011.
[33] J.W. Taylor, L.M. De Menezes, P.E. McSharry, A comparison of univariate methods for forecasting electricity demand up to a day ahead, Int. J. Forecast. 22 (1) (2006) 1–16.
[34] S. Kim, H. Kim, A new metric of absolute percentage error for intermittent demand forecasts, Int. J. Forecast. 32 (3) (2016) 669–679.
[35] H. Pham, A new criterion for model selection, Mathematics 7 (2019) 1–12.
[36] M.T. Hagan, H.B. Demuth, M. Beale, Neural Network Design, PWS Publishing Co., 1997.
[37] H. Konno, H. Yamazaki, Mean-absolute deviation portfolio optimization model and its applications to Tokyo stock market, Manag. Sci. 37 (5) (1991) 519–531.
[38] V. V Spichak, Estimating temperature distributions in geothermal areas using a neuronet approach, Geothermics 35 (2) (2006) 181–197.
[39] M. Mehri, M. Ghazaghi, A hybrid model of uniform design and artificial neural network for the optimization of dietary metabolizable energy, digestible lysine, and methionine in quail chicks, Brazilian J. Poult. Sci. 16 (3) (2014) 313–318.
[40] R.E. Caraka, S.A. Bakar, M. Tahmid, H. Yasin, I.D. Kurniawan, Neurocomputing fundamental climate analysis, Telkomnika 17 (4) (2019) 1818–1827.